ABC effect and resonance structure in the double-pionic fusion to ³He

P. Adlarson,[1,*] W. Augustyniak,[2] W. Bardan,[3] M. Bashkanov,[4,5] F. S. Bergmann,[6] M. Berłowski,[7] H. Bhatt,[8] A. Bondar,[9,10] M. Büscher,[11,12,†] H. Calén,[1] I. Ciepał,[3] H. Clement,[4,5,‡] D. Coderre,[11,12,13,§] E. Czerwiński,[3] K. Demmich,[6] E. Doroshkevich,[4,5] R. Engels,[11,12] A. Erven,[14,12] W. Erven,[14,12] W. Eyrich,[15] P. Fedorets,[11,12,16] K. Föhl,[17] K. Fransson,[1] F. Goldenbaum,[11,12] P. Goslawski,[6] A. Goswami,[11,12,18] K. Grigoryev,[11,12,19,¶] C.-O. Gullström,[1] F. Hauenstein,[15] L. Heijkenskjöld,[1] V. Hejny,[11,12] B. Höistad,[1] N. Hüsken,[6] L. Jarczyk,[3] T. Johansson,[1] B. Kamys,[3] G. Kemmerling,[14,12] F. A. Khan,[11,12] A. Khoukaz,[6] D. A. Kirillov,[20] S. Kistryn,[3] H. Kleines,[14,12] B. Kłos,[21] W. Krzemień,[3] P. Kulessa,[22] A. Kupść,[1,7] A. Kuzmin,[9,10] K. Lalwani,[8,‖] D. Lersch,[11,12] B. Lorentz,[11,12] A. Magiera,[3] R. Maier,[11,12] P. Marciniewski,[1] B. Mariański,[2] M. Mikirtychiants,[11,12,13,19] H.-P. Morsch,[2] P. Moskal,[3] H. Ohm,[11,12] I. Ozerianska,[3] E. Perez del Rio,[4,5] N. M. Piskunov,[20] P. Podkopał,[3] D. Prasuhn,[11,12] A. Pricking,[4,5] D. Pszczel,[1,7] K. Pysz,[22] A. Pyszniak,[1,3] J. Ritman,[11,12,13] A. Roy,[18] Z. Rudy,[3] S. Sawant,[8,11,12] S. Schadmand,[11,12] T. Sefzick,[11,12] V. Serdyuk,[11,12,23] B. Shwartz,[9,10] R. Siudak,[22] T. Skorodko,[4,5,24] M. Skurzok,[3] J. Smyrski,[3] V. Sopov,[16] R. Stassen,[11,12] J. Stepaniak,[7] E. Stephan,[21] G. Sterzenbach,[11,12] H. Stockhorst,[11,12] H. Ströher,[11,12] A. Szczurek,[22] A. Täschner,[6] A. Trzciński,[2] R. Varma,[8] G. J. Wagner,[4] M. Wolke,[1] A. Wrońska,[3] P. Wüstner,[14,12] P. Wurm,[11,12] A. Yamamoto,[25] L. Yurev,[23,#] J. Zabierowski,[26] M. J. Zieliński,[3] A. Zink,[15] J. Złomańczuk,[1] P. Żuprański,[2] and M. Żurek[11,12]

(WASA-at-COSY Collaboration)

[1]*Division of Nuclear Physics, Department of Physics and Astronomy, Uppsala University, Box 516, 75120 Uppsala, Sweden*
[2]*Department of Nuclear Physics, National Centre for Nuclear Research, ul. Hoza 69, 00-681, Warsaw, Poland*
[3]*Institute of Physics, Jagiellonian University, ul. Reymonta 4, 30-059 Kraków, Poland*
[4]*Physikalisches Institut, Eberhard-Karls-Universität Tübingen, Auf der Morgenstelle 14, 72076 Tübingen, Germany*
[5]*Kepler Center für Astro- und Teilchenphysik, Physikalisches Institut der Universität Tübingen,*
Auf der Morgenstelle 14, 72076 Tübingen, Germany
[6]*Institut für Kernphysik, Westfälische Wilhelms-Universität Münster, Wilhelm-Klemm-Straße 9, 48149 Münster, Germany*
[7]*High Energy Physics Department, National Centre for Nuclear Research, ul. Hoza 69, 00-681, Warsaw, Poland*
[8]*Department of Physics, Indian Institute of Technology Bombay, Powai, Mumbai 400076, Maharashtra, India*
[9]*Budker Institute of Nuclear Physics of SB RAS, 11 Akademika Lavrentieva Prospect, Novosibirsk, 630090, Russia*
[10]*Novosibirsk State University, 2 Pirogova Street, Novosibirsk, 630090, Russia*
[11]*Institut für Kernphysik, Forschungszentrum Jülich, 52425 Jülich, Germany*
[12]*Jülich Center for Hadron Physics, Forschungszentrum Jülich, 52425 Jülich, Germany*
[13]*Institut für Experimentalphysik I, Ruhr-Universität Bochum, Universitätsstraße 150, 44780 Bochum, Germany*
[14]*Zentralinstitut für Engineering, Elektronik und Analytik, Forschungszentrum Jülich, 52425 Jülich, Germany*
[15]*Physikalisches Institut, Friedrich-Alexander-Universität Erlangen-Nürnberg, Erwin-Rommel-Straße 1, 91058 Erlangen, Germany*
[16]*Institute for Theoretical and Experimental Physics, State Scientific Center of the Russian Federation,*
25 Bolshaya Cheremushkinskaya, Moscow, 117218, Russia
[17]*II. Physikalisches Institut, Justus-Liebig-Universität Gießen, Heinrich-Buff-Ring 16, 35392 Giessen, Germany*
[18]*Department of Physics, Indian Institute of Technology Indore, Khandwa Road, Indore 452017, Madhya Pradesh, India*
[19]*High Energy Physics Division, Petersburg Nuclear Physics Institute, 2 Orlova Rosha, Gatchina, Leningrad District, 188300, Russia*
[20]*Veksler and Baldin Laboratory of High Energiy Physics, Joint Institute for Nuclear Physics, 6 Joliot-Curie, Dubna, 141980, Russia*
[21]*August Chełkowski Institute of Physics, University of Silesia, Uniwersytecka 4, 40-007, Katowice, Poland*
[22]*The Henryk Niewodniczański Institute of Nuclear Physics, Polish Academy of Sciences, 152 Radzikowskiego Street, 31-342 Kraków, Poland*
[23]*Dzhelepov Laboratory of Nuclear Problems, Joint Institute for Nuclear Physics, 6 Joliot-Curie, Dubna, 141980, Russia*
[24]*Department of Physics, Tomsk State University, 36 Lenina Avenue, Tomsk, 634050, Russia*
[25]*High Energy Accelerator Research Organisation KEK, Tsukuba, Ibaraki 305-0801, Japan*
[26]*Department of Cosmic Ray Physics, National Centre for Nuclear Research, ul. Uniwersytecka 5, 90-950 Łódź, Poland*

Exclusive and kinematically complete measurements of the double pionic fusion to ³He have been performed in the energy region of the so-called ABC effect, which denotes a pronounced low-mass enhancement in the $\pi\pi$-invariant mass spectrum. The experiments were carried out with the WASA detector setup at COSY (the cooler synchrotron at Forschungszentrum Jülich). Similar to the observations in the basic $pn \to d\pi^0\pi^0$ reaction and in the $dd \to {}^4\text{He}\,\pi^0\pi^0$ reaction, the data reveal a correlation between the ABC effect and a resonance-like energy dependence in the total cross section. Differential cross sections are well described by the hypothesis of d^* resonance formation during the reaction process in addition to the conventional t-channel $\Delta\Delta$ mechanism. The deduced d^* resonance width can be understood from collision broadening due to Fermi motion of the nucleons in initial and final nuclei.

I. INTRODUCTION

Historically the so-called ABC effect, which denotes an intriguing low-mass enhancement in the $\pi\pi$ invariant mass spectrum, is known from inclusive measurements of two-pion production in reactions where the participating nucleons fuse to the few-body systems d, ^{3}He, and ^{4}He, respectively. In the respective literature such reactions have been termed double-pionic fusion reactions. The ABC effect has been named after the initials of Abashian, Booth, and Crowe, who were the first to observe this effect in 1960 by studying the inclusive $pd \to {}^3$He X reaction [1]. Its explanation has been a puzzle since then. In subsequent bubble-chamber [2,3] and single-arm magnetic spectrometer measurements [4–12] this enhancement was observed also in double-pionic fusion reactions leading to d, ^{3}He, and ^{4}He, if an isoscalar pion pair was produced. However, such an enhancement was not observed in fusion reactions leading to deuteron and triton, if an isovector pion pair was produced.

These results led to the conclusion that this effect only appears in reactions where the participating nucleons fuse to a nuclear bound system in the final state in combination with the production of an isoscalar pion pair.

In recent exclusive and kinematically complete measurements of the $pn \to d\pi^0\pi^0$ reaction it has been demonstrated [13–15] that the ABC effect in this basic double-pionic fusion reaction is correlated with a narrow structure in the total cross section with quantum numbers $I(J^P) = 0(3^+)$, a mass of 2.37 GeV, and a width of about 70 MeV. The mass is about 90 MeV below $2m_\Delta$, the mass of a $\Delta\Delta$ system, and the width is three times narrower than expected from a conventional t-channel $\Delta\Delta$ process.

In contrast, the basic isovector fusion process $pp \to d\pi^+\pi^0$ exhibits neither an ABC effect nor a narrow resonance structure [13,16] in agreement with the observations in all other pp initiated two-pion channels [17–21]. Isospin decomposition of all three reactions $pn \to d\pi^0\pi^0$, $pn \to d\pi^+\pi^-$, and $pp \to d\pi^+\pi^0$ leading to the double-pionic fusion of deuterium ensured that the resonance structure is of purely isoscalar nature [13]. Also recently published data on the $pn \to pp\pi^0\pi^-$ reaction show evidence for the resonance structure, though in this case of an isovector pion pair the ABC

effect is absent [22]. Compelling evidence that the isoscalar resonance structure observed in two-pion production processes denotes truly an s-channel resonance in the pn system comes from polarized np scattering in the energy region of the ABC effect [23,24]. Inclusion of these data in the SAID (Scattering Analysis Interactive Dial-in) database with subsequent partial-wave analysis produces a pole at $(2380 \pm 10 - i40 \pm 5)$ MeV in the coupled $^3D_3$-$^3G_3$ partial waves, in full agreement with the resonance hypothesis discussed here.

Since in these latter reactions the resonance is not associated with any ABC effect, it was no longer called ABC resonance, but d^* [22]—in historical reference to a predicted [25,26] dibaryon with exactly the quantum numbers as we observe it now.

The existence of the ABC effect in the double-pionic fusion to ^{3}He and ^{4}He has been confirmed by exclusive and kinematically complete experiments at CELSIUS/WASA [27,28] and recently also at ANKE-COSY [29]. In measurements at WASA-at-COSY it has been additionally shown that in the $dd \to {}^4$He $\pi^0\pi^0$ reaction the ABC effect is again correlated with a resonance structure in the total cross section at $\sqrt{s} \approx 2.37$ GeV $+ 2m_N$ [30]. However, in comparison to the basic fusion reaction to deuterium the width of the resonance structure appears substantially broadened, which may be attributed to the Fermi motion of the nucleons in initial and final nuclei as well as due to collision damping.

So what is left in this scenario is the question of whether also in case of the double-pionic fusion to ^{3}He the ABC effect is correlated with a resonance structure in the total cross section.

II. EXPERIMENT

In an effort to find an experimental answer for this question we have analyzed corresponding two-pion production data, which were obtained with WASA at COSY [31,32]. The data sets, which we used, originate from two different runs.

The first run concerns a proton beam of energy $T_p = 1.0$ GeV hitting the deuterium pellet target [31,32]. This allows us to analyze the reaction $pd \to {}^3$He $\pi^0\pi^0$ at $T_p = 1.0$ GeV. The beam energy corresponds to a center-of-mass (c.m.) energy of $\sqrt{s} = 3.42$ GeV $= 2.48$ GeV $+ m_N$, i.e., pertains to the high-energy end of the region, where the ABC effect has been observed previously [1–3,27].

The second data set used for our purposes concerns runs with a deuteron beam of $T_d = 1.4$ and 1.7 GeV, respectively, hitting the deuterium pellet target. We use these runs to obtain data for the quasifree reaction $dd \to {}^3$He $\pi^0\pi^0 + n_{spectator}$ in the range $3.1 < \sqrt{s} < 3.4$ GeV (with respect to the ^{3}He $\pi^0\pi^0$ system), i.e., covering just the ABC region.

Both data sets allow an exclusive and kinematically complete reconstruction of the ^{3}He $\pi^0\pi^0$ events with kinematic overconstraints.

The trigger for a valid event was just a single track in the forward detector of WASA with high thresholds in its first scintillation detector layers, in order to suppress fast protons and deuterons. With this trigger condition the data rate of accepted events was at moderate 2 kHz. The selection criteria for the offline analysis were a single He track in the forward detector and four neutral hits in the central detector.

*Present address: Institut für Kernphysik, Johannes Gutenberg-Universität Mainz, Johann-Joachim-Becher Weg 45, 55128 Mainz, Germany.

†Present address: Peter Grünberg Institut, PGI-6 Elektronische Eigenschaften, Forschungszentrum Jülich, 52425 Jülich, Germany and Institut für Laser- und Plasmaphysik, Heinrich-Heine Universität Düsseldorf, Universitätsstraße 1, 40225 Düsseldorf, Germany.

‡Corresponding author: clement@pit.physik.uni-tuebingen.de

§Present address: Albert Einstein Center for Fundamental Physics, Universität Bern, Sidlerstraße 5, 3012 Bern, Switzerland.

‖Present address: III. Physikalisches Institut B, Physikzentrum, RWTH Aachen, 52056 Aachen, Germany.

¶Present address: Department of Physics and Astrophysics, University of Delhi, Delhi 110007, India.

#Present address: Department of Physics and Astronomy, University of Sheffield, Hounsfield Road, Sheffield, S3 7RH, United Kingdom.

The emerging ^{3}He particles were registered in the forward detector of WASA and identified by the ΔE-E technique. The photons from the π^0 decay were detected and identified in the central detector [31]. Consequently four-momenta were measured for all emitted particles of an event with the exception of the spectator neutron, which appears in the second reaction type only.

Together with the condition that two pairs of the detected photons have to fulfill the π^0 mass condition, we have six overconstraints for the kinematic fit of an event in the first reaction type and three overconstraints in the second case. From the three possible combinations to reconstruct the four-momenta of the two pions out of four photon signals the one with the smallest χ^2 has been selected [19,30].

All particles have been detected over the full solid angle with the exception of those ^{3}He ejectiles, which escaped in the beam pipe (polar angles $\Theta_{^3He}^{lab} < 3°$).

Acceptance and efficiency corrections have been made by use of Monte Carlo (MC) simulations of detector setup and performance. For a self-consistent procedure the reaction model used in the MC simulations has been iteratively adjusted to the experimental results.

With regard to the second data set the momentum spectra of the reconstructed neutron are shown in Fig. 1, at the top for $T_d = 1.4$ GeV and at the bottom for $T_d = 1.7$ GeV. The strong enhancement of events at low momenta corresponds to the situation when the spectator neutron originates from the target deuteron, whereas the enhancement at the high-momentum end corresponds to a spectator neutron stemming from a beam deuteron. The area in between is covered by non-quasifree processes, so-called coherent processes, where the reconstructed neutron is not just a kinematic spectator, but also plays an active role in the reaction dynamics. Misidentified ^{4}He particles could be eliminated in subsequent analysis steps by the constraint that the reconstructed neutron should not have the same direction and velocity as the detected He particle.

In case of a target spectator neutron (dp reaction) the emitted ^{3}He particles are at very small forward angles due to the Lorentz boost, so that the lower limit of $\Theta_{lab} \geqslant 3°$ cuts severely into the reaction phase space rendering acceptance corrections largely model dependent. Hence we refrain from giving results for this scenario.

For the case of the neutron spectator originating from the beam deuteron (pd reaction) the situation is kinematically much more favorable. Unfortunately also here we met difficulties, since the energies of the ^{3}He ejectiles deposited in the segments of the forward detector turned out to be partly below the trigger thresholds, which were increased for the observation of other reaction channels of primary interest in these runs. As a consequence we had to tune the actual trigger thresholds individually for each of the detector segments very carefully by adjusting the simulations of the detector performance to the observed response of each of the corresponding scintillation detectors.

Comparing the spectra in Fig. 1, top and bottom, we see that at higher beam energy the coherent process has much reduced compared to the quasifree process. Hence, also in this respect it is more favorable to analyze the 1.7 GeV data for the ^{3}He $\pi^0\pi^0$ production channel.
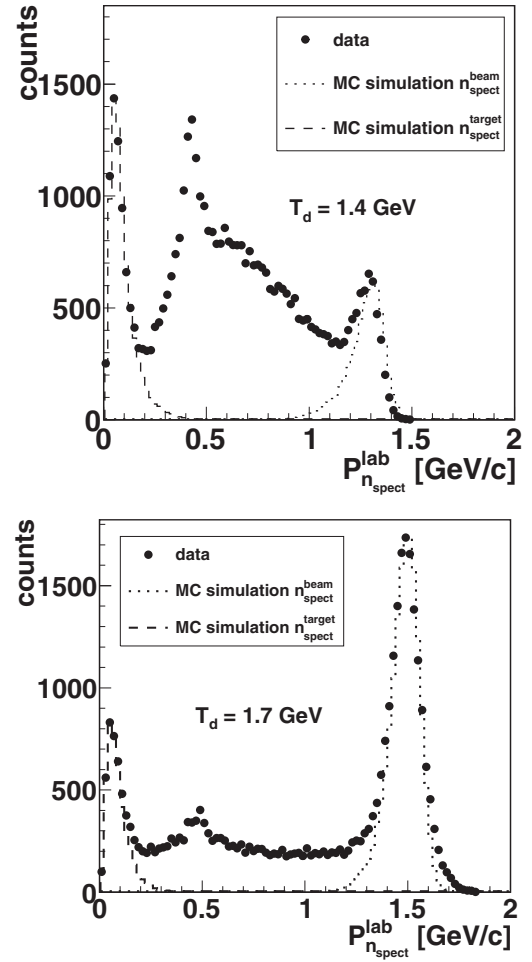

FIG. 1. Distribution of the reconstructed neutron momenta in the $dd \to {}^3He\,\pi^0\pi^0 + n$ reaction at $T_d = 1.4$ GeV (top) and 1.7 GeV (bottom), respectively. Data are given by solid dots. The dashed (dotted) lines show the expected distribution for the quasifree process based on the CD Bonn potential [33] deuteron wave function, if the spectator originates from the target (beam) deuteron. The peak near 0.5 GeV/c originates from ^{4}He contamination, which has been removed in subsequent analysis steps.

Figure 2 displays the two-dimensional scatter plot of the kinetic energy of the ^{3}He ejectile versus its polar scattering angle in the laboratory system. The ^{3}He particles originating from the quasifree process in the target deuteron (dp reaction) produce a strong enhancement at small angles in combination with large kinetic energies in the scatter plot, whereas the ^{3}He ejectiles from the quasifree process in the beam deuteron (pd reaction) produce a strong enhancement at small energies over a wide region of angles. In the scatter plot these two regions are strongly populated and well separated from the region in between, which covers coherent processes. In order to get rid of the latter as well as of the target related spectators, we subsequently constrain the polar angle for the reconstructed neutrons to the kinematical spectator limit of $\Theta_n^{c.m.} \leqslant 11.5°$ for beam related spectators, where the superscript $c.m.$ denotes the angle in the dp center-of-mass system. That way we obtain a momentum spectrum of the spectator neutrons, which is very
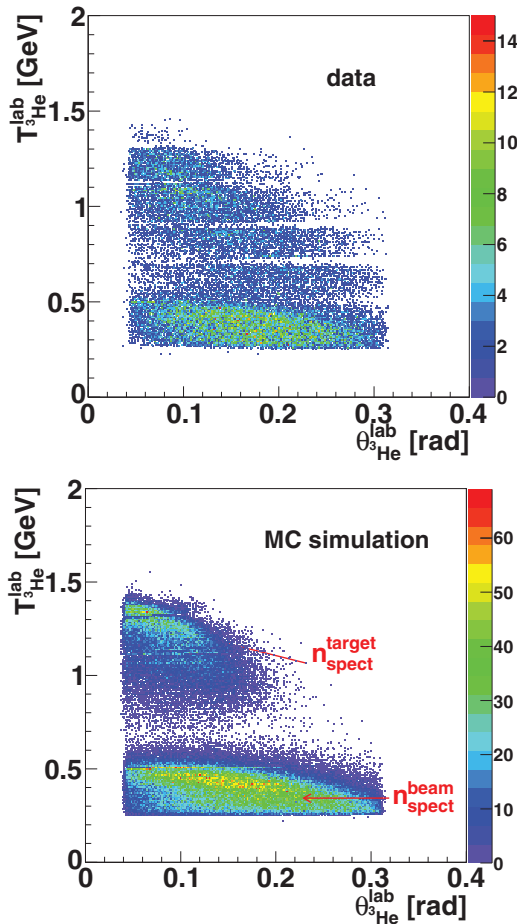
FIG. 2. (Color online) Scatter plot of the kinetic energy of the ^{3}He ejectiles in the $dd \rightarrow {}^3\text{He}\,\pi^0\pi^0 + n$ reaction at $T_d = 1.7$ GeV versus the ^{3}He laboratory scattering angle $\Theta_{{}^3\text{He}}^{lab}$. At the top data are shown and at the bottom the corresponding MC simulation of the processes with either the neutron spectator in the target or in the beam. The high-density area at small angles and large kinetic energies corresponds to the process with the spectator neutron in the target, whereas the distribution at small energies and large scattering angles belongs to spectator neutrons in the beam. The area in between corresponds to coherent processes.

close to that given by the dotted line in Fig. 1 and which is essentially free of background.

The absolute normalization of the data from the single-energy measurement at $T_p = 1.0$ GeV was obtained by a relative normalization to the $pd \rightarrow {}^3\text{He}\,\pi^0$ reaction measured simultaneously with the same trigger. Our results for this reaction in turn have been normalized to those from Saclay measurements at neighboring energies [34,35]. Though this procedure appears to be straightforward, it contains a number of difficulties. The Saclay data appear to be most reliable at $\Theta_{{}^3\text{He}} = 180°$ [34], where WASA cannot measure. Hence we used the full back-angle hemisphere to adjust the WASA results to those of Saclay. However, due to the scarcity of Saclay data at finite angles we estimate that the total uncertainty in the absolute normalization could be as large as 30%. For details see Ref. [36].
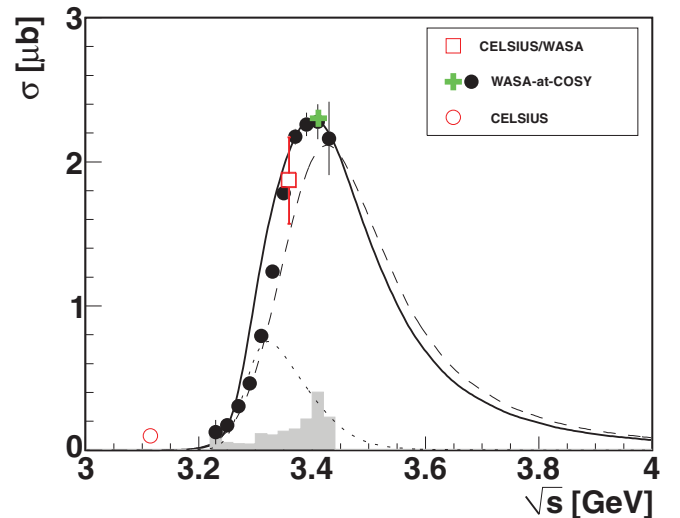

FIG. 3. (Color online) Energy dependence of the total cross section for the double-pionic fusion to ^{3}He with the production of a $\pi^0\pi^0$ pair. Data obtained in this work by measurements of the $pd \rightarrow {}^3\text{He}\,\pi^0\pi^0$ reaction at $T_p = 1.0$ GeV and of the $dd \rightarrow {}^3\text{He}\,\pi^0\pi^0 + n_{spectator}$ reaction at $T_d = 1.7$ GeV are given by the filled cross and the filled circles, respectively. They are compared to previous results from PROMICE/WASA [37] (open circle) and CELSIUS/WASA [27] (open square). The latter has been renormalized; see text. The shaded area denotes the estimated systematic uncertainties. The dotted curve gives the d^* contribution, the dashed line the t-channel $\Delta\Delta$ process, and the solid line their (coherent) sum.

The data of the quasifree run overlap with the single-energy measurement at their high-energy end. Hence, for simplicity they have been normalized to the result of the single-energy measurement.

III. RESULTS

Resulting observables of the normalized as well as acceptance and efficiency corrected data are displayed in Figs. 3–6.

The total cross section data obtained from the analysis of both experiments are shown in Fig. 3, which exhibits the energy dependence of the total cross section for the ${}^3\text{He}\,\pi^0\pi^0$ production. Our result from the run at $T_p = 1.0$ GeV ($\sqrt{s} = 3.416$ GeV) is shown by the filled cross symbol, whereas the results from the quasifree run are given by the filled circles. The shaded area denotes the estimated systematic uncertainties, which result dominantly from the efficiency and acceptance corrections. Also uncertainties from rest gas contributions and kinematic fit are contained in this estimate.

Included in Fig. 3 are also the results from previous exclusive measurements at CELSIUS-WASA at $T_p = 0.893$ GeV (open square) [27] and at PROMICE/WASA at $T_p = 0.477$ GeV (open circle) [37], the latter carried out at CELSIUS too.

In order to avoid systematic discrepancies in the procedure used for the absolute normalization, the CELSIUS-WASA result has been reanalyzed by subjecting it to exactly the same procedure (i.e., considering the full back-angle hemisphere) as applied now for the single-energy measurement at $T_p = 1.0$ GeV. As a result the CELSIUS-WASA value at
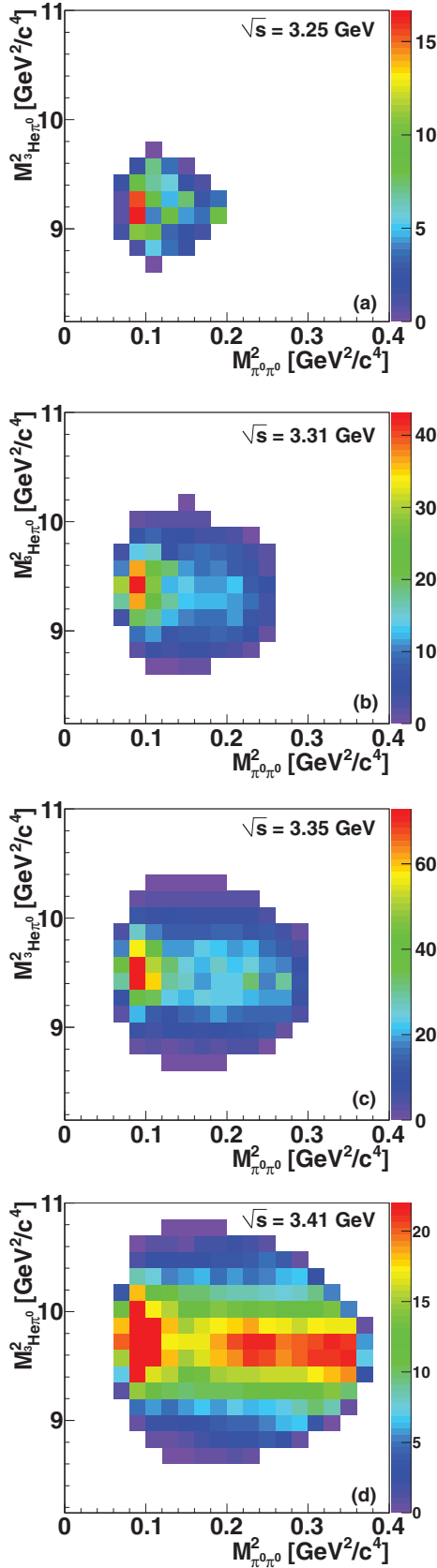
FIG. 4. (Color online) Dalitz plots of $M^2_{^3He\pi^0}$ versus $M^2_{\pi^0\pi^0}$ of the data at c.m. energies of $\sqrt{s} = 3.25$ GeV, $\sqrt{s} = 3.31$ GeV, $\sqrt{s} = 3.35$ GeV, and $\sqrt{s} = 3.41$ GeV (from top to bottom).
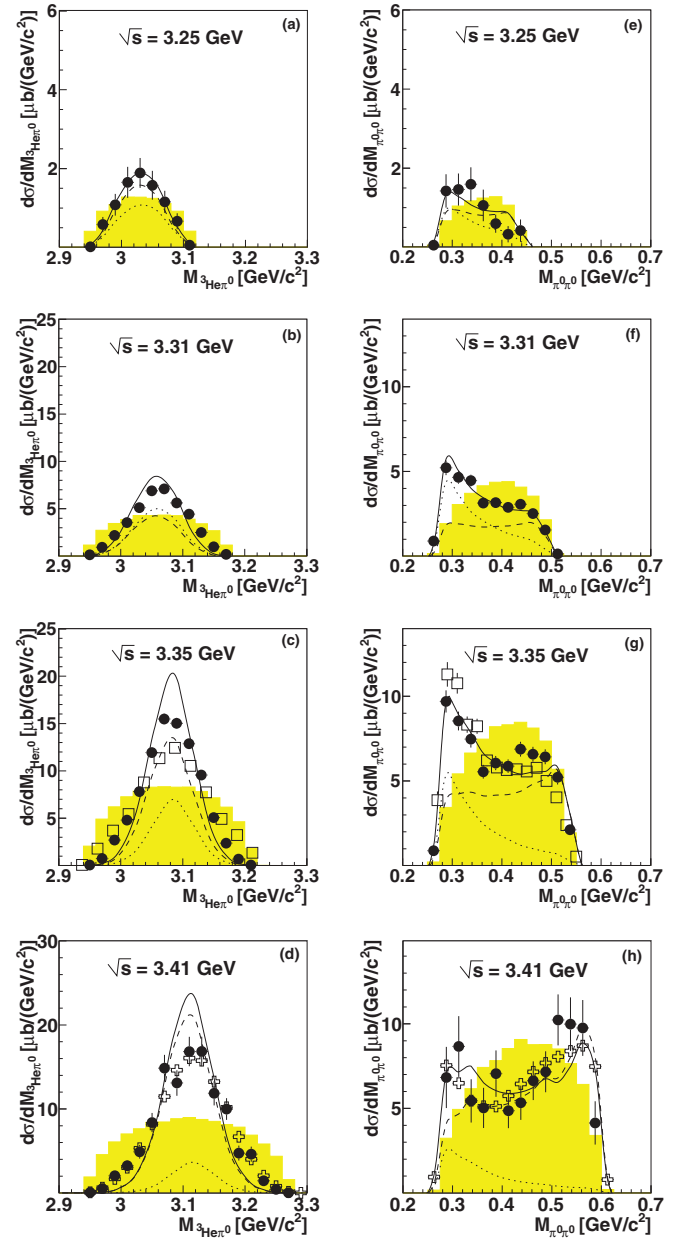

FIG. 5. (Color online) Distributions of $M_{^3He\pi^0}$ (left) and $M_{\pi^0\pi^0}$ (right) at $\sqrt{s} = 3.25$, 3.31, 3.35 and 3.41 GeV (from top to bottom). Filled circles denote data from the quasifree runs, open crosses those from the pd reaction at $T_p = 1.0$ GeV ($\sqrt{s} = 3.416$ GeV). Data from CELSIUS/WASA at $T_p = 0.89$ GeV ($\sqrt{s} = 3.35$ GeV) [27] are shown by open squares. The shaded area denotes the phase-space distribution. The dotted curve gives the d^* contribution, the dashed line the t-channel $\Delta\Delta$ process and the solid line their sum.

$T_p = 0.893$ GeV changed from the published value of 2.8(3) μb [15] to 1.9(3) μb with the latter value being plotted in Fig. 3. The revised value is in good agreement with the new data. We note that the COSY-ANKE result for the $pd \rightarrow {}^3$He $\pi^+\pi^-$ reaction is also lower by 40% [29], when compared to the corresponding published value from CELSIUS-WASA, in agreement with our finding for the ^{3}He $\pi^0\pi^0$ channel.
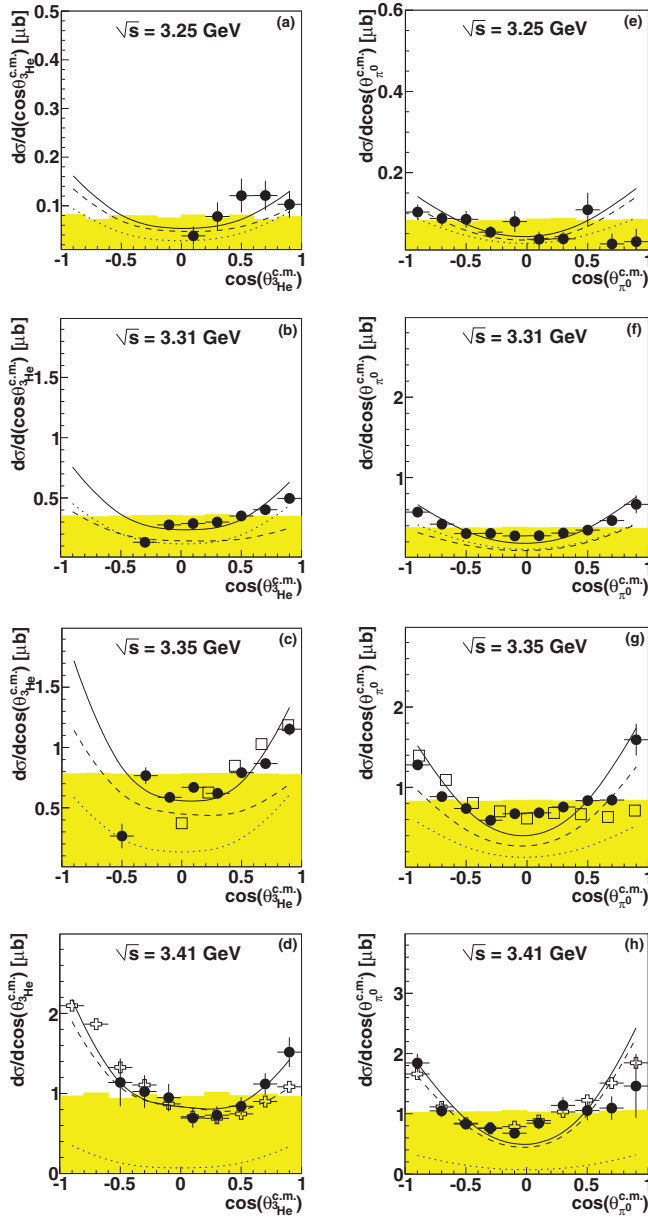
FIG. 6. (Color online) Same as Fig. 5, but for the angular distributions of ^{3}He (left) and π^0 (right) ejectiles in the center-of-mass system.

For sake of completeness we note that there is also a COSY-MOMO measurement of the ^{3}He $\pi^+\pi^-$ channel at 70 MeV above threshold, i.e., at $\sqrt{s} = 3.16$ GeV [38]. From the observed $M_{\pi^+\pi^-}$ distributions it was concluded that the produced $\pi^+\pi^-$ pair is dominantly in relative p wave, i.e., of isovector character [38,39], which is excluded in the $\pi^0\pi^0$ system discussed here.

The energy dependence of the total cross section is consistent with some resonance-like structure, though we do not observe a substantial decrease of the cross section at high energies within the measured interval. The cross section appears to peak at a similar excess energy as was observed in the fusion reactions to deuterium and ^{4}He. However, as

the detailed investigation of the differential cross sections will show, the d^* resonance at $\sqrt{s} = 2.37$ GeV $+ m_N$ shows up in the total cross section only as a shoulder within the ascending slope. In marked difference to the double-pionic fusions to d and ^{4}He, the main contribution to the total cross section in the ^{3}He case does not originate from the d^* resonance, but from the conventional t-channel $\Delta\Delta$ process, which has a large isovector contribution. This process peaks at around $2m_\Delta + m_N$ and has a width of about $2\Gamma_\Delta$ [13,16].

Next we discuss the differential cross sections, which are shown in Figs. 4–6 and which completely describe the three-body reaction. The shape of all differential distributions remains rather stable over the region of the d^* resonance structure, but starts to change significantly towards the high-energy end of the measured region, where the t-channel $\Delta\Delta$ process becomes dominant.

Figure 4 shows the variation of the Dalitz plots for the invariant masses squared $M^2_{^3\text{He}\,\pi^0}$ versus $M^2_{\pi^0\pi^0}$ over the measured resonance region. The Dalitz plots are similar to those obtained in the basic reaction. They exhibit an enhancement in horizontal direction, in the region of the Δ excitation, as it prominently shows up in the $M_{^3\text{He}\,\pi^0}$ spectra displayed in Fig. 5. This feature is consistent with the excitation of a $\Delta\Delta$ system in the intermediate state, as discussed for the basic reaction [14,15]. More prominent—and also similar to the situation in the basic reaction—we observe here the ABC effect as a strong enhancement at the low-mass kinematic limit of $M_{\pi^0\pi^0}$. Consequently the Dalitz plot is mainly populated along the $\pi\pi$ low-mass border line.

In Fig. 5, left, the $M_{^3\text{He}\,\pi^0}$ distribution is shown for four selected energies over the measured region. At all energies this distribution is far from phase-space-like (shaded areas in Fig. 5) and exhibits a clear signal from Δ excitation.

The $M_{\pi^0\pi^0}$ distribution is shown on the right-hand side of Fig. 5 for four different beam energies. It clearly exhibits the ABC effect at the lower three energies. At the highest energy we see the transition to a two-hump structure with both a low-mass enhancement and a high-mass enhancement. The latter is the characteristic feature of the t-channel $\Delta\Delta$ process as predicted originally by Risser and Shuster [40] in search for a plausible explanation of the ABC effect.

In Fig. 6 we show angular distributions at the selected energies. On the left the angular distribution of the ^{3}He ejectiles is depicted and on the right that of the emitted π^0 particles—both in the center-of-mass system. Since the collision partners are not identical particles, the c.m. angular distributions do not need to be symmetric about 90°. However, in case of an s-channel resonance process they have to be symmetric, and the data appear to be compatible with this.

The observed ^{3}He angular dependence is similar to the corresponding one in the basic reaction, though significantly more peaked near $\cos\Theta = \pm 1$. However, the angular distribution is still less curved than in the case of the double-pionic fusion to ^{4}He.

The π^0 angular distribution resembles that for p waves as one would expect from the decay of Δs in the intermediate state. Note that an intermediate $\Delta\Delta$ system shows up both in the case of d^* excitation and in the case of a t-channel meson exchange leading to a mutual excitation of the colliding

nucleons to their first excited state, the Δ resonance (t-channel $\Delta\Delta$ process).

Since the features, which we observe here, are very similar to those observed for the basic double-pionic fusion reaction, we adapt the ansatz used there for the description of the ^{3}He case [14]. There are only two major differences:

1. First, the nucleons' momenta are smeared due to their Fermi motion in initial and final nuclei. In particular the Fermi motion in the appreciably bound ^{3}He nucleus leads to a sizable smearing of the energy dependence in the total cross section adding nearly 30 MeV to the total width.
2. Second, the reaction process $pd \rightarrow\, ^3$He $\pi^0\pi^0$ involves also the proton within the target deuteron, which does not participate actively in the formation of the pn resonance, but finally forms a bound ^{3}He system together with the pn pair from the decay of the d^* resonance.

The results of this calculation is shown in Figs. 3, 5, and 6 by the solid lines, which provide a reasonable description of the data. In these calculations it is assumed that both the d^* resonance and the t-channel $\Delta\Delta$ process happen on the active pn pair. The $\Delta\Delta$ process is of both isoscalar and isovector character. From isospin coupling it follows that the latter is more than three times as large [36]. Since only the isoscalar part of the $\Delta\Delta$ process interferes with d^*, the interference effect between both processes is small. The relative size of both processes as well as the width of d^* resonance has been adjusted for best reproduction of the observed $M_{\pi^0\pi^0}$ distributions. The resulting effective d^* width of 85 MeV means that there is—if at all—only a small broadening due to collision damping. It is appreciably smaller than in the ^{4}He case, where the collision broadening was about 50 MeV.

The result of the fit to the $M_{\pi^0\pi^0}$ spectra has been scaled in absolute height to the total cross section data in Fig. 3. We see that the d^* resonance dominates only at low energies in the strongly ascending part of the total cross section. Thereafter the conventional t-channel $\Delta\Delta$ process takes over.

From Fig. 3 we see that the maximum cross section for d^* production in the process $pd \rightarrow d^*p \rightarrow\, ^3$He $\pi^0\pi^0$ is about 0.8 μb. This is a factor of 300 less than in the basic reaction $pn \rightarrow d^* \rightarrow d\pi^0\pi^0$, but also about a factor of 2 less than in the process $dd \rightarrow d^*np \rightarrow\, ^4$He $\pi^0\pi^0$, where there are twice as many combinatoric possibilities to form d^* in the intermediate state. This result suggests that the d^* production in still heavier nuclei does not just fade away, but rather could give sizable contributions.

In view of the now achieved understanding of the double-pionic fusion it appears historically rather fortunate that more than fifty years ago the Berkeley 184-inch synchrocyclotron allowed only a maximum proton beam energy of 743 MeV. That way Abashian, Booth, and Crowe were in the position to just enter the energy region where the $\pi\pi$ low-mass enhancement appears to be largest—and thus discover the ABC effect. Would they have had access to a beam energy of 1 GeV instead, they would then have observed both a low-mass and a high-mass enhancement, with the latter being

the dominant one. But such a scenario was readily explained later on by Risser and Shuster [40] to originate naturally from the conventional t-channel $\Delta\Delta$ process. Would thus the ABC puzzle have escaped detection without later providing the trace to the discovery of the d^* resonance?

IV. CONCLUSIONS AND OUTLOOK

In conclusion, our data on the double-pionic fusion process to ^{3}He establish the correlation of a resonance-like energy dependence in the total cross section with the ABC effect in very much the same way as shown before for the double-pionic fusion reactions to deuterium and ^{4}He. A calculation based on the d^* resonance gives a good account of the observed distributions. The enlarged width of the resonance structure in the total cross section is explained by the Fermi motion of the nucleons in initial and final nuclei, which includes also collision damping.

That way the ABC effect in the double-pionic fusion to nuclei is traced back to a pn resonance, which obviously is strong enough to survive even in the nuclear medium. It would be very interesting to see whether also in nuclei heaver than He both ABC effect and d^* resonance could be observed. Since the next heavier nuclei are not stable or do not have the proper spin and isospin, the next suitable candidate reaction appears to be d^{14}N $\rightarrow\, ^{16}$O $\pi\pi$ or in inverse kinematics ^{14}N $d \rightarrow$ ^{16}O $\pi\pi$. However, measurements of such reactions necessitate dedicated detector setups and/or accelerators. Another great possibility to search for the ABC effect and d^* resonance might be given by high-resolution measurements of heavy-ion reactions.

A trace that d^* production, indeed, takes place in heavy-ion collisions has recently been found in connection with the so-called DLS puzzle, which denotes an unusual enhancement in the e^+e^- production at $0.3 \lesssim M_{e^+e^-} \lesssim 0.7$ GeV initiated by neutron-proton collisions in vacuum or within heavy-ion systems. In Ref. [41] it has been shown that a possible solution of this puzzle is presented by accounting for $\Delta\Delta$ and d^* production.

Since a dibaryon resonance has integer spin and thus is of bosonic nature, the survival of such a resonance in a nuclear surrounding may have an important impact on the equation of state. Bosons are not Pauli blocked and as such allow for higher densities under same pressure and energy conditions. The behavior of matter under extreme conditions is needed, e.g., for a better understanding of the evolution of compressed matter in the course of heavy-ion collisions or in compact (neutron) stars; see, e.g., Refs. [42–45].

[1] N. E. Booth, A. Abashian, and K. M. Crowe, Phys. Rev. Lett. **7**, 35 (1961); **5**, 258 (1960); Phys. Rev. **132**, 2296 (1963).
[2] I. Bar-Nir *et al.*, Nucl. Phys. B **54**, 17 (1973).
[3] A. Abdivaliev *et al.*, Sov. J. Nucl. Phys. **29**, 796 (1979).
[4] R. J. Homer *et al.*, Phys. Lett. **9**, 72 (1964).
[5] J. H. Hall *et al.*, Nucl. Phys. B **12**, 573 (1969).
[6] J. Banaigs *et al.*, Phys. Lett. B **43**, 535 (1973).
[7] J. Banaigs *et al.*, Nucl. Phys. B **67**, 1 (1973).
[8] J. Banaigs *et al.*, Nucl. Phys. B **105**, 52 (1976).
[9] F. Plouin *et al.*, Nucl. Phys. A **302**, 413 (1978).
[10] F. Plouin, P. Fleury, and C. Wilkin, Phys. Rev. Lett. **65**, 690 (1990).
[11] R. Wurzinger *et al.*, Phys. Lett. B **445**, 423 (1999).
[12] For a review see A. Codino and F. Plouin, Report No. LNS/Ph/94-06 (unpublished).
[13] P. Adlarson *et al.*, Phys. Lett. B **721**, 229 (2013).
[14] P. Adlarson *et al.*, Phys. Rev. Lett. **106**, 242302 (2011).
[15] M. Bashkanov *et al.*, Phys. Rev. Lett. **102**, 052301 (2009).
[16] F. Kren *et al.*, Phys. Lett. B **684**, 110 (2010); **702**, 312(E) (2011).
[17] H. Clement, Prog. Part. Nucl. Phys. **67**, 486 (2012).
[18] T. Skorodko *et al.*, Phys. Lett. B **695**, 115 (2011).
[19] P. Adlarson *et al.*, Phys. Lett. B **706**, 256 (2012).
[20] T. Skorodko *et al.*, Phys. Lett. B **679**, 30 (2009).
[21] T. Skorodko *et al.*, Eur. Phys. J. A **47**, 108 (2011).
[22] P. Adlarson *et al.*, Phys. Rev. C **88**, 055208 (2013).
[23] P. Adlarson *et al.*, Phys. Rev. Lett. **112**, 202301 (2014).
[24] P. Adlarson *et al.*, Phys. Rev. C **90**, 035204 (2014).
[25] T. Goldman, K. Maltman, G. J. Stephenson, K. E. Schmidt, and F. Wang, Phys. Rev. C **39**, 1889 (1989).
[26] J. L. Ping, H. X. Huang, H. R. Pang, F. Wang, and C. W. Wong, Phys. Rev. C **79**, 024001 (2009).
[27] M. Bashkanov *et al.*, Phys. Lett. B **637**, 223 (2006).
[28] S. Keleta *et al.*, Nucl. Phys. A **825**, 71 (2009).
[29] M. Mielke *et al.*, Eur. Phys. J. A **50**, 102 (2014).
[30] P. Adlarson *et al.*, Phys. Rev. C **86**, 032201(R) (2012).
[31] Chr. Bargholtz *et al.*, Nucl. Instrum. Methods A **594**, 339 (2008).
[32] H. H. Adam *et al.*, arXiv:nucl-ex/0411038.
[33] R. Machleidt, Phys. Rev. C **63**, 024001 (2001).
[34] C. Kerboul *et al.*, Phys. Lett. B **181**, 28 (1986).
[35] J. Banaigs *et al.*, Phys. Lett. B **45**, 394 (1973).
[36] E. Perez del Rio, Ph.D. thesis, University of Tübingen, 2014, http://hdl.handle.net/10900/53837.
[37] M. Andersson *et al.*, Phys. Lett. B **485**, 327 (2000).
[38] F. Bellemann *et al.*, Phys. Rev. C **60**, 061002 (1999).
[39] G. Fäldt, A. Gardestig, and C. Wilkin, Phys. Lett. B **496**, 185 (2000).
[40] T. Risser and M. D. Shuster, Phys. Lett. B **43**, 68 (1973).
[41] M. Bashkanov and H. Clement, Eur. Phys. J. A **50**, 107 (2014).
[42] M. I. Krivoruchenko *et al.*, Phys. At. Nucl. **74**, 371 (2011).
[43] R. M. Aguirre and M. Schvellinger, Phys. Lett. B **449**, 161 (1999).
[44] A. Faessler, A. J. Buchmann, and M. I. Krivoruchenko, Phys. Rev. C **57**, 1458 (1998).
[45] A. W. Thomas, D. L. Whittenbury, J. D. Carroll, K. Tsushima, and J. R. Stone, EPJ Web Conf. **63**, 03004 (2013).